Modeling and Simulation of a Ground Based Sense and Avoid Architecture for Unmanned Aircraft System Operations

Kyle R. Noth[1] and Daniel W. Luke[2]
The MITRE Corporation, Bedford, MA, 01730

The safe operation of Unmanned Aircraft Systems in the National Airspace System necessitates a capability to sense and avoid other airborne objects. One solution is a Ground Based Sense and Avoid concept, where data from ground-based radars are fused in a specially tuned tracking system that can provide traffic information to manual (flight crews) or automatic collision avoidance systems. In this paper, we will present a modeling and simulation approach for assessing site-specific radar detection and tracking performance. High fidelity primary surveillance radar and tracking system models enable simulation studies with the objective of determining target probability of detection and distributions of expected track initiation times across the surveillance volume. Atmospheric and environmental conditions, terrain, and land coverage type affect radar wave propagation. Models take into account these sources of degradation, as well as target characteristics, site-specific radar performance, and tracking system filtering and initiation logic. This information will help in the development of a GBSAA concept of operation, mission planning, and will ultimately define where UAS can operate with sufficient surveillance performance to meet sense and avoid requirements.

I. Introduction

THE safe operation of Unmanned Aircraft Systems (UAS) in the National Airspace System (NAS) requires a capability to sense and avoid other airborne targets. One candidate solution is a Ground Based Sense and Avoid (GBSAA) architecture, which leverages existing ground radar systems to detect other airborne objects. A tracking system fuses available radar surveillance information and provides traffic information to the flight crew or an automated collision avoidance system. Current research efforts include assessing system performance on detecting pop-up, non-cooperative (non-transponding) airborne objects, and the resultant ability to form valid tracks from the detections. The track initiation time of a target is dependent on site-specific radar coverage performance and tracker filtering and initiation logic. We are using modeling and simulation to assist in the development of a GBSAA concept of operation, mission planning, and ultimately identifying airspace volumes where radar surveillance performance is sufficient to enable UAS operations within the NAS using GBSAA.

The radar system infrastructure in the United States is a critical national asset providing surveillance information for air traffic management (ATM), weather observation, border protection, and homeland security. Our focus is on the performance of a radar's primary surveillance mode (PSR) to detect non-cooperative targets. Radar detection performance is strongly influenced by site dependent environmental factors such as terrain, land coverage and atmospheric conditions and therefore must be accurately modeled to predict real world performance. Simulation of the radar and fusion tracking algorithms enables us to determine target detection and tracking performance of different target types with surveillance information fused from multiple heterogeneous and asynchronous radar systems. This capability allows us to evaluate the feasibility of using ground-based radars for a variety of applications, including Unmanned Aircraft System (UAS) sense and avoid. As part of this article, we will present our modeling and simulation approach, discuss our analytical methods for evaluating radar performance, and provide a short discussion of recent field data collections in the vicinity of Edwards Air Force Base, CA to validate the simulation models and detection predictions.

[1] Senior Multi-Disciplinary System Engineer, 202 Burlington Rd. Bedford, MA 01730
[2] Lead Sensor System Engineer, 202 Burlington Rd. Bedford, MA 01730

II. Background and Motivation

Aircraft detection and tracking in the National Airspace System are accomplished by using both primary and secondary surveillance techniques enabled by the Airport Surveillance Radars (ASR) and Air Route Surveillance Radars (ARSR) (Nolan, 2011). These systems are jointly owned and operated by the Federal Aviation Administration (FAA) and the Department of Defense (DoD). Non-cooperative airborne objects such as gliders, balloons, ultra lights, and some general aviation (GA) aircraft present a big challenge to a sense and avoid system. The GBSAA concept leverages the PSR mode of existing ASR and ARSR assets for the detection of these potential non-cooperative collision threats. The simulation methodology described here will help determine the site-specific surveillance performance and safe UAS operational volumes where potential non-cooperative threats can be sensed and appropriate avoidance procedures executed in a timely manner.

The DoD has identified the use of ground based radar systems as a viable solution for enabling UAS operations in the NAS. Currently, UAS operations in the NAS are highly restricted due to a lack of a see and avoid capability. Federal Aviation Regulations (FAR's) require that "regardless of whether an operation is conducted in VFR or IFR, vigilance shall be maintained… so as to see and avoid other aircraft…" (Federal Aviation Administration, 2010). The FAA issues Certificates of Authorization (COA) to the DoD and the Department of Homeland Security (DHS) for limited operation of UAS in domestic airspace (Austin, 2010). Operations approved through the COA process require ground observers, a chase airplane, or an equivalent means for the see and avoid requirement outside of positively controlled airspace. Due to the operational restrictions placed on the UAS when operating under a COA, a less constraining solution for sense and avoid that will allow for routine UAS access to the NAS is highly desirable.

While several different architectural concepts may prove to be successful in providing a sense and avoid capability, the present research is motivated by the development of a specific implementation of a GBSAA architecture that leverages existing air traffic control radar assets already fielded across the NAS. The Ground Based Sense and Avoid architecture, illustrated in Figure 1, relies on ATC and/or tactical radar systems to detect airborne targets. A tracking system correlates and fuses the primary and secondary surveillance data from all of the participating radar systems. The tracker drives a modified display system to provide a single integrated picture of the airspace traffic to the UAS flight crew. The pilot will maneuver the UAS to remain well clear from all airborne traffic (Weibel, et al., 2011). Appropriate separation standards between UAS' and airborne targets depend on time allocations for the sense and avoid encounter timeline, illustrated in Figure 2, and may vary based on different sense and avoid architecture solutions and UAS performance and maneuverability. The sense and avoid encounter timeline considers the time required to detect and track an intruder, evaluate the collision potential, prioritize the collision hazard, determine an appropriate avoidance maneuver, and the time required to command and execute the maneuver (Federal Aviation Administration, 2009). Appropriately modeling each of these functions provides much insight into the overall sense and avoid requirement. Results will contribute to the definition of appropriate separation standards and the further refinement of concepts of operation. There will be a voice communication link between the Ground Control Station (GCS) and ATC for coordination between the UAS flight crew and ATC. Appropriate coordination procedures with ATC will be in place in the event that the UAS operator needs to deviate from ATC instruction to avoid other aircraft.

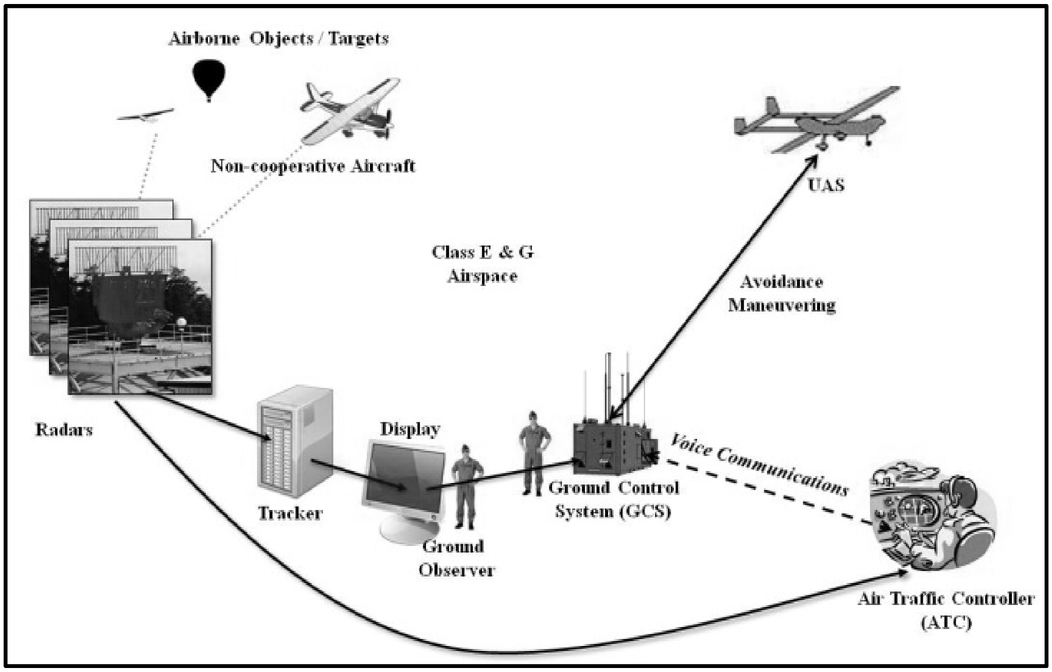

Figure 1: Ground Based Sense and Avoid (GBSAA) Architecture

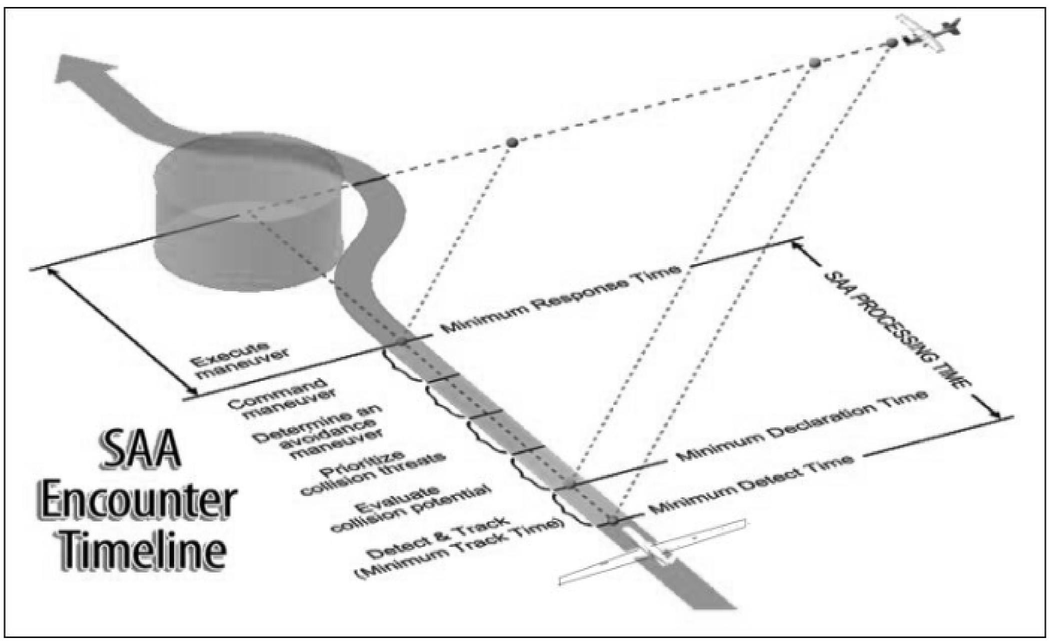

Figure 2: Sense and Avoid Encounter Timeline for Collision Avoidance (Federal Aviation Administration, 2009)

One major hurdle to overcome in the GBSAA concept of operations is quantifying the site-specific performance and dynamics of the different systems. Of particular interest is the performance of the surveillance systems: the radar and tracker family of systems. The sense and avoid encounter timeline is predicated on successfully detecting and tracking the target intruder. Appropriate modeling and simulation studies evaluate the effectiveness of the GBSAA architecture in performing these functions. If the intruder is not successfully tracked with sufficient time and distance from the UAS to satisfy the sense and avoid encounter timeline functions, a collision could be imminent. Therefore, high confidence in the detection and tracking of aeronautical hazards is of critical importance for the safety of the GBSAA solution. The UAS must be operated only in areas where radar detection performance is sufficient for meeting the detection and tracking requirements. In addition, airborne targets that penetrate the radar coverage floor pose a high risk for a near mid-air collision (NMAC) because they may pop-up in close proximity to the UAS. If the intruder pop-up occurs within the distance required for the UAS to complete the sense and avoid encounter timeline, a collision could be imminent. For the safe operation of UAS' in the NAS, the UAS must operate at a safe altitude above the radar coverage floor such that intruding aircraft can be sufficiently tracked with sufficient time and distance to avoid a collision risk.

III. Modeling and Simulation Approach

Modeling and simulation techniques provide an appropriate avenue for exploring system performance in detecting and tracking airborne targets. The performance and dynamics of the radar and tracker under real world site-specific conditions, coupled with the generation of intruder targets, are simulated to evaluate the time required for the radar and tracking system to detect and initiate track on an airborne target. The resulting simulation data will enable us to quantitatively map out safe airspace volumes for UAS operations at any given site within the NAS.

The overall modeling and simulation approach is summarized in Figure **3**. The modeling of the different radar systems and an airspace traffic characterization in the concerned operational volume are completed as a pre-process. In the simulation environment, aircraft targets are generated from aircraft performance and operating characteristics distributions. We simulate track initiation and maintenance for each target by the tracking model, which receives target detection information from heterogeneous and asynchronous radar systems. As the signal from a given radar is reflected off the aircraft target, the likelihood of detecting the target is precisely the probability of detection (P_d) at that location for the given radar system, as determined by the radar performance model. Results from the modeling and simulation environment include statistical distributions of target detection, track initiation, and track maintenance performance parameters.

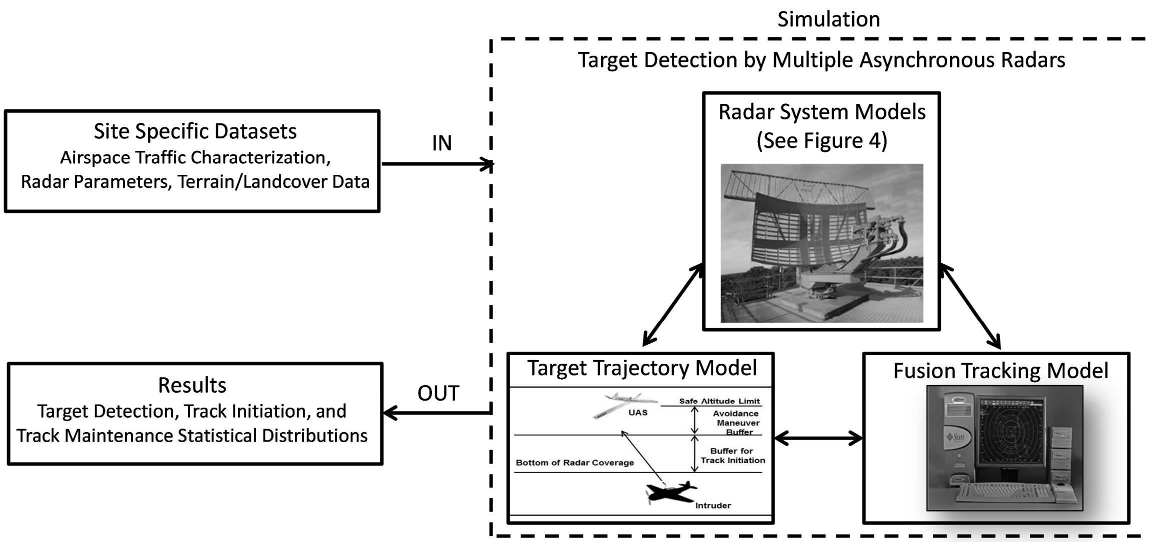

Figure 3: Aircraft detection and tracking modeling and simulation approach

A. Radar System Modeling

The Advanced Refractive Effects Prediction System (AREPS), a radar simulation tool developed by the Space and Navy Warfare Systems Command (SPAWAR) (Space and Naval Warefare Systems Center (SPAWAR), 2010), is the backbone of our radar modeling capability. In AREPS, we calculate the probability of detecting a target with a specified Radar Cross Section (RCS) by appropriately specifying radar performance parameters and site-specific terrain and land coverage characteristics. The AREPS Advanced Propagation Model (APM) uses terrain data, land coverage reflectivity information, atmospheric models, and appropriate electromagnetic wave propagation models to determine radar line-of-sight, multipath effects, atmospheric refraction, land cover reflectivity and absorption, and other propagation effects on radar performance (Space and Naval Warefare Systems Center (SPAWAR), 2010). Simulation results are in the form of Signal-to-Noise (SNR) and target P_d as a function of RCS, Probability of False Alarm (P_{fa}) and location relative to the radar.

Enhanced supplementary models that we have developed allow us to characterize with higher fidelity the site-specific factors affecting the radar system. Our enhanced models include a capability to evaluate radar operating characteristic trades, perform trade studies on tracking system logic and filtering settings, assess the P_d for a target of any RCS, as well as the ability to visualize radar system dynamics and detection performance. Each of the model enhancements is discussed in more detail in subsequent sections of this paper. Figure 4 illustrates the overall technical radar modeling approach.

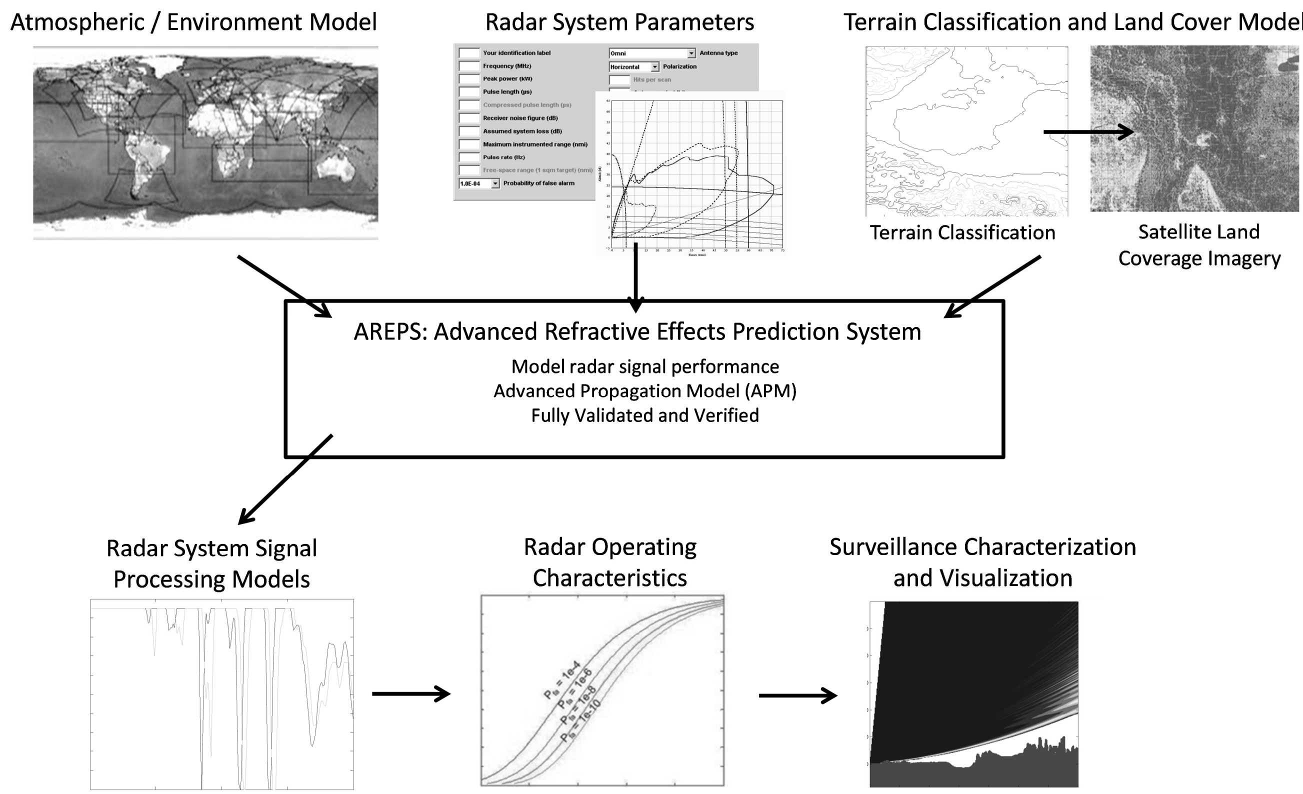

Figure 4: Radar system modeling approach

1. Radar Detection Fundamentals

Airport surveillance radars provide terminal radar coverage near major airports and areas with high traffic density. Due to the widespread deployment of the ASR-11 system for terminal area surveillance, and its potential for enabling GBSAA for UAS operations in the NAS, the focus of this article will rely on the modeling and simulation of that system. The DoD and the FAA have a joint program for the procurement of the ASR-11 and Standard Terminal Automation Replacement System (STARS). These radar and tracking/display systems are deployed strategically around the United States to provide radar surveillance at over 200 locations. It is important to note that the generic modeling approach that we will present applies to all types of radars, but platform specific models are needed to accurately characterize radar system performance.

Primary radar systems emit energy through the transmitter feedhorn. This signal will propagate freely through the atmosphere until it hits a target, at which point the signal is reflected back to the receiver. The receiver input consists of both the radar echo signal, and assumed zero mean Gaussian noise (Skolnik, 2008). Detection of targets in noise, due to the random variance of the noise echo, is a statistical process with a P_d of less than unity and a P_{fa} of greater than zero (Richards, et al., 2010). There is a compromise between achieving a high P_d and maintaining an acceptably low P_{fa}. The desired system P_{fa} is the driver to establishing the detection threshold. The threshold is set based on observed signal interference in the absence of targets, caused by external noise, clutter, and other environmental effects (Richards, et al., 2010) (O'Donnell, 2010).

Derviation of mathematical expressions for P_d and P_{fa} as a function of Signal-to-Noise Ratio (SNR) are dependent on the assumptions made regarding the characteristics of the noise, the type of target, and the integration type of the radar. Without digressing into these derivations, we will point the interested reader to the relevant sources (Richards, et al., 2010) (Mahafza, et al., 2004) (Skolnik, 1990). Applying the results of these well exercised derivations leads directly to the development of analytical models for establishing the valuable relationships between RCS and SNR, P_d, and P_{fa}.

2. Radar Wave Propagation Modeling

The Signal-to-Interference ratio (SIR) ultimately expresses the radar detection performance. If the return signal (S) from a target is sufficiently higher in magnitude than the sum of the different sources of interference, detection is declared. Sources of interference include thermal noise (N), clutter (C), and jamming (J). For the purpose of this research, we assume that jamming is negligible since frequency spectrum analysis during radar siting minimizes the influence of unintentional jamming. We assume that the use of active jamming systems is rare within domestic airspace. With this assumption, the sources of interference of concern can be expressed in the familiar context of Signal-to-Noise Ratio (SNR) and Clutter-to-Noise Ratio (CNR). The SNR, more commonly referred to as the radar equation, is the governing equation of radar performance. The CNR differs from the SNR only in that the target radar cross section, σ_t, is replaced by the surface clutter cross section, σ_c, as indicated in Eq. 1 and Eq. 2.

$$SNR = \frac{P_t G^2 \lambda^2 \sigma_t}{(4\pi)^3 R^4 k T_o B F L} \tag{1}$$

$$CNR = \frac{P_t G^2 \lambda^2 \sigma_c}{(4\pi)^3 R^4 k T_o B F L} \tag{2}$$

where the term P_t is the peak transmission power, G is the power gain for the transmitter and the receiver antennae (assumed to be the same), λ is the radar wavelength, and σ is the target RCS. In the denominator, R is the range from the radar to the target (assuming a monostatic radar system), k is Boltzmann's constant, T_o is the system noise temperature, B is the effective noise bandwidth, F is the radar noise figure, and L is a term to capture all system losses. Subsequent sections in this paper discuss, in detail, calculation of the SNR and CNR, and hence a comprehensive assessment of the signal-to-interference ratio.

3. Advanced Propagation Model (APM)

For our modeling efforts, we use the Advanced Propagation Model (APM) in AREPS to calculate SIR throughout the entire surveillance volume. APM is a hybrid approach that combines four sub-models for radar wave propagation: flat earth, ray optics, extended optics, and split-step parabolic equations (Space and Naval Warefare Systems Center (SPAWAR), 2010) (Skolnik, 2008). The sub-models are applied in appropriate regions of the radar coverage space to achieve a good compromise between computation time and fidelity. The APM merges the Radio Physical Optics (RPO) and Terrain Parabolic Equation Model (TPEM) (Space and Naval Warefare Systems Center (SPAWAR), 2010), models for gaseous absorption, and surface clutter (Skolnik, 2008). For more detailed information on APM, please consult Skolnik (3rd Ed) (Skolnik, 2008) and Navy publications on the development and employment of their modeling approach (Space and Naval Warfare Systems Center, Pacific Atmospheric Propagation Branch (5548), 2009).

4. Impact of Terrain and Land Cover

Local terrain and land cover represent undesirable interference sources that cumulatively degrade the radar's ability to detect a target. Terrain acts as a source of interference in several ways, including terrain obscuration and multipath generation. In addition, when the radar beam illuminates a ground patch, backscattering from the local terrain and land cover generates unwanted echoes (i.e. radar clutter). The strength of the radar clutter return is dependent on the characteristics of the landform and land cover. AREPS has a built-in capability to model these local environmental factors and analyze their effect on the radar detection performance. We have developed an automated method for creating accurate site-specific land cover/landform characterization data that can be imported into the AREPS model.

The two dominant sources of terrain-related interference accounted for in the APM are terrain obscuration and multipath. Terrain obscuration occurs when the radar line-of-sight to the target is blocked by intervening terrain. Multipath results when a transmitted signal arrives at the target along two paths. Multipath is a particularly strong source of interference for ground-based radars trying to detect low flying airborne targets near the earth's surface, a target class of particular interest in this paper. The local terrain is characterized using the National Geospatial Intelligence Agency's (NGA) Digital Terrain Elevation Data (DTED) and the US Geological Survey's (USGS) National Elevation Dataset (NED).

Figure 5 (a) and (b) show the AREPS predicted performance for an ASR-11 located at Edwards AFB and Grand Forks AFB, respectively. Each plot represents height vs. range P_d contours using the ASR-11 low beam antenna pattern against an assumed target RCS of $1m^2$ at a specific azimuth relative to the radar. In Figure 5(a) the effects of terrain masking, caused by the San Gabriel Mountains, are apparent. Figure 5(b) represents the low beam coverage of the Grand Forks AFB ASR-11 at an azimuth of 10°. The surrounding terrain at Grand Forks is characterized by flat plains. The effects of multipath are evident by the alternating lobe maximum and null pattern observed, with respect to elevation angle, at the lower altitudes near the range coverage boundary in Figure 5(b).

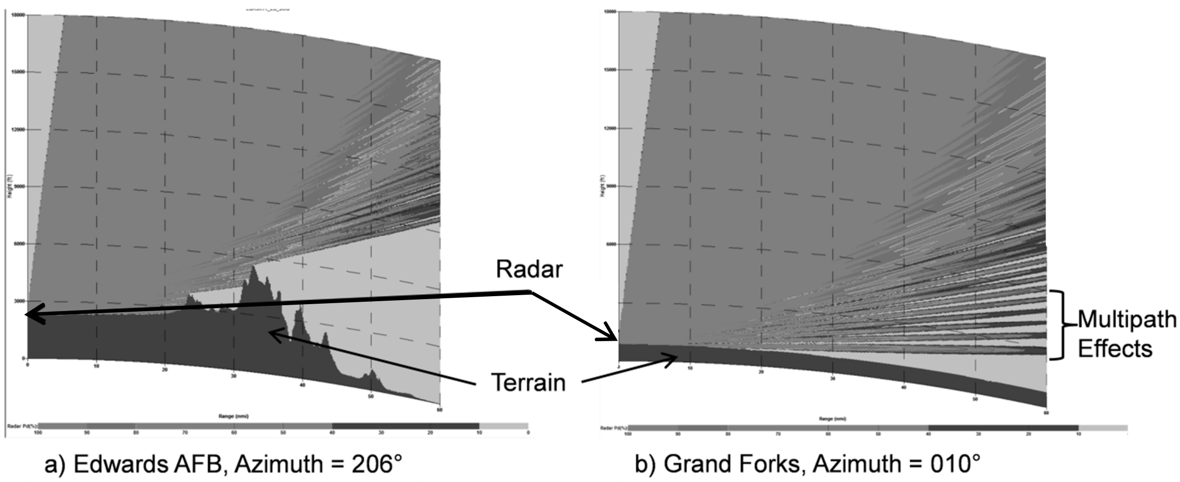

Figure 5: ASR-11 low beam P_d coverage for $1m^2$ RCS target a) at Edwards AFB and b) at Grand Forks AFB

The effects of site-specific land clutter returns on the signal-to-interference ratio, and hence the probability of target detection, are accounted for in AREPS by the computation of the clutter-to-noise ratio. The APM calculates the clutter power based on radar frequency, polarization, angle of incidence of the illuminating beam with the surface (grazing angle), and land cover/landform type (e.g. forest, croplands, mountains, etc.) (Space and Naval Warfare Systems Center, Pacific Atmospheric Propagation Branch (5548), 2009). The term in the radar equation that determines the magnitude of the clutter return strength is embodied in the clutter cross section, σ_c, which is the product of the reflectivity coefficient associated with the land surface type and the area of the clutter cell illuminated by the radar. The reflectivity coefficient depends on the land surface characteristics determined by the land cover and landforms lying within the radar's coverage volume. This includes the grazing angle and the surface scatter effectiveness, which is a function of the land cover type and surface roughness (flat or mountainous terrain). Different types of land cover have different associated surface scatter effectiveness. For example, mountain and urban areas, wooded/rolling hills, tree and bush cover, farmland/crops, and flatlands like desert, grassland and marshy terrain all have different surface scatter effectiveness.

For our application, where the radar range of interest can extend beyond 60 nautical miles, we would have to populate 400,000 data points to accurately model the landform/cover type for a given site, assuming a 100 m range data resolution increment and an azimuth resolution increment of 1 deg. Therefore, the production of an accurate site-specific landform/cover type clutter map for the APM is a manually intensive process. We have developed an automated GIS-based technique to populate an AREPS compatible database that accurately characterizes the land clutter environment at any specific location within the US.

The USGS makes available a comprehensive US land cover database (as a GeoTIFF image file) called the National Land Cover Database (NLCD) (Homer et al., 2012) derived primarily from Landsat 7 imagery that is updated on a 5 year cycle (latest publicly available database is NLCD2006). Although the NLCD does not explicitly account for seasonal variations (e.g., crop lands transitioning to a fallow state in winter) which would impact ground clutter returns, we have a capability to override the NLCD land category type at any data pixel point with any other user desired NLCD land category to allow for a known current land cover state. Each pixel in the GeoTIFF file is both geo-referenced and color coded with information associated with the land cover type as illustrated in Figure 6

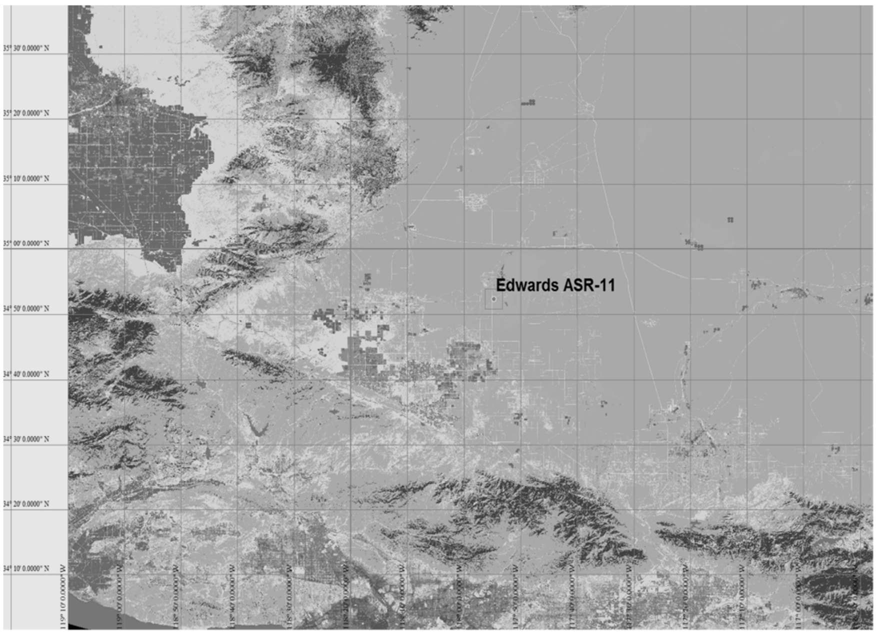

NLCD 2001 Class Code		NLCD 2001 Description
11		Open Water
12		Perennial Ice, Snow
21		Developed, Open Space
22		Developed, Low Intensity
23		Developed, Medium Intensity
24		Developed, High Intensity
31		Barren Land, Rock, Sand, Clay
32		Unconsolidated Shore*
31		Barren Land, Rock, Sand, Clay
31		Barren Land, Rock, Sand, Clay
31		Barren Land, Rock, Sand, Clay
41		Deciduous Forest
42		Evergreen Forest
43		Mixed Forest
51		Dwarf Scrub**
52		Shrub, Scrub
71		Grassland, Herbaceous
72		Sedge, Herbaceous**
73		Lichens**
74		Moss**
81		Pasture, Hay
82		Cultivated Crops
82		Cultivated Crops
82		Cultivated Crops
21		Developed, Open Space
90		Woody Wetlands
95		Emergent Herbaceous Wetlands
91		Palustrine Forested Wetland*
92		Palustrine Scrub/Shrub Wetland*
93		Estuarine Forested Wetland*
94		Estuarine Scrub/Shrub Wetland*
96		Palustrine Emergent Wetland*
97		Estuarine Emergent Wetland*
98		Palustrine Aquatic Bed*
99		Estuarine Aquatic Bed*

Figure 6: National Land Cover Database (NDCL2001) for Edwards AFB region

Image processing of the NLCD data files provides us with an accurate one arc-second by one arc-second resolution latitude and longitude grid of land cover types in the area of interest. These land cover types are then mapped to the equivalent AREPS land cover classes and their associated scatter effectiveness values and used to automatically generate an AREPS-compatible land cover database. However, the NLCD database only provides information on site-specific land cover without any indication of the underlying landform (e.g., mountains, plains, etc.). This lack of information poses a problem for accurately determining land clutter returns since mountains are one of the largest contributors to radar land clutter. Therefore, we need an algorithm to automatically classify terrain to accurately model the effects of land clutter.

The landform modeling approach, originated by Wood (Wood, 1996), is used to develop an automated mountain land type classification technique based on the high-resolution USGS 1 arc-second NED digital elevation data. Wood's technique analyzes the surface convexity along the direction of minimum and maximum profile convexity over a local region and classifies the landform into six categories: *peak, ridge, pass, plane, channel and pit.* Wood's classification algorithm (Wood, 1996) is based on a series of second partial derivative tests (in two directions) that quantify the degree of convexity to determine the appropriate landform category. A set of inference rules based on the frequency of occurrence of ridges, channels, passes and planes were developed to automatically decide whether an areal subset is mountainous. The techniques described above have been adapted for use in specifying the AREPS terrain files automatically to account for the presence of mountainous terrain.

This high-fidelity and automated algorithm development enables us to evaluate the impact of terrain and land cover on radar signal-to-interference ratio, and hence radar target detection performance, at any site with relative ease and quick turn-around.

5. Model Application: (Digital Airport Surveillance Radar (DASR/ASR-11)

While the generic radar modeling approach discussed thus far can be applied to any monostatic radar system, platform specific models are needed to fully account for operating mode dynamics and signal processing techniques. The ASR-11, which is the radar system used for our GBSAA concept, is a Moving Target Detector (MTD), constant false alarm rate (CFAR), track-while-scan (TWS), primary surveillance radar (Raytheon Corporation, 2011). Additionally, the ASR-11 has a monopulse secondary surveillance radar (MSSR) system, used to detect and track cooperative aircraft through transponder interrogation. The PSR has two feedhorns for a switchable high/low beam, which provides improved target detection through clutter mitigation. There are four separate coherent processing intervals (CPIs) for each the high and low beam, with five pulses per CPI, at staggered pulse repetition frequencies (PRFs) and with frequency cycling (Raytheon Corporation, 2011). The use of multiple CPIs at different frequencies and PRFs can provide information for target radial velocity determination (Skolnik, 1990). Frequency diversity and cycling are useful for mitigating rain attenuation and the effects of various sources of interference such as multipath and ground clutter.

The return received from one CPI is processed in a bank of 5-pulse finite-impulse-response filters (Skolnik, 1990). Coherent integration increases the SNR thereby reducing the single pulse SNR required for a given P_d. After one CPI is received, the PRF is staggered and the RF frequency is changed slightly, at which point another CPI of five pulses in transmitted. The use of different PRFs on successive coherent dwells helps eliminate blind speeds (Skolnik, 1990). Doppler filters are used to suppress clutter. The output from the Doppler filter goes through the envelope detector and is subsequently processed through the cell-averaging CFAR processor (Skolnik, 1990). The four CPIs are processed through a configurable "*M of N*" binary integrator, which is typically set to 2 out of 4 detections (Raytheon Corporation, 2011). This integration scheme requires that at least *M* of the *N* coherently integrated pulse trains has a positive detection to declare a target detection. The use of binary integration enhances target detection performance while reducing false alarms, thereby enhancing target track performance.

For radars that have multiple beams and/or multiple frequencies, separate AREPS runs for each beam and/or frequency is needed to accurately represent the performance of the radar system. Appropriately combining the SNR for each of the beams at each of the frequencies requires a detailed understanding of the design and operation of the radar system. Significant performance benefits result from overlapping coverage provided by multiple beams and frequencies. P_d nulls that exist at one frequency are slightly displaced from those at the other frequency, effectively reducing the presence of the voids. Multiple radar beams operating at different elevation angles effectively reduces the presence of ground clutter on the radar display.

While the baseline ASR-11 switches back and forth between the high and low beam, Raytheon is currently testing a concurrent beam processing (CBP) technique, which will allow for the simultaneous use of both the high beam and the low beam. Initial field results demonstrate improved clutter mitigation and increased P_d. In addition, Raytheon is experimenting with algorithms for using the amplitude difference between the high and low beam for altitude estimation of non-cooperative targets; hence making the 2D ASR-11 a 3D radar system (Drake, 2011), (Drake et al., 2009).

In the simulation environment, the probability of a radar detecting a target intruder during each radar update is precisely the radar P_d at the given location of the intruding airborne object. The radar system model provides P_d as a function of location relative to the radar for a given target RCS and P_{fa}. This radar detection performance information is used in the larger simulation environment.

6. Validation and Verification

AREPS has been fully validated and accredited by SPAWAR and is an approved application within the Department of the Navy Chief Information Officer Applications & Database Management System and the North Atlantic Treaty Organization (NATO) (EM Propagation Modeling and System Performance Assessment by SPAWARSYSCEN San Diego, 2007). The APM used by AREPS is the only accredited EM propagation model (EM Propagation Modeling and System Performance Assessment by SPAWARSYSCEN San Diego, 2007). Both AREPS and APM are elements of the Defense Modeling and Simulation Office (DMSO) library (EM Propagation Modeling and System Performance Assessment by SPAWARSYSCEN San Diego, 2007).

The ASR-11 model was developed in cooperation with Raytheon as part of a Cooperative Research and Development Agreement (CRADA). Radar detection performance determined by our models is consistent with the data provided by Raytheon. Raytheon's high and low beam vertical coverage pattern for the ASR-11 corresponding to a $P_d \geq 0.8$, $P_{fa} = 10^{-6}$ and target RCS of $1m^2$ is shown in Figure 7(a). The P_d predictions generated from our radar modeling toolset for the same case are compared to the Raytheon high and low beam vertical coverage in Figure 7(b) and 6(c), respectively. There is strong agreement for the 80% P_d contour as a function of range and altitude relative to the radar location between the model results and the Raytheon vertical coverage diagram (Drake et al., 2009).

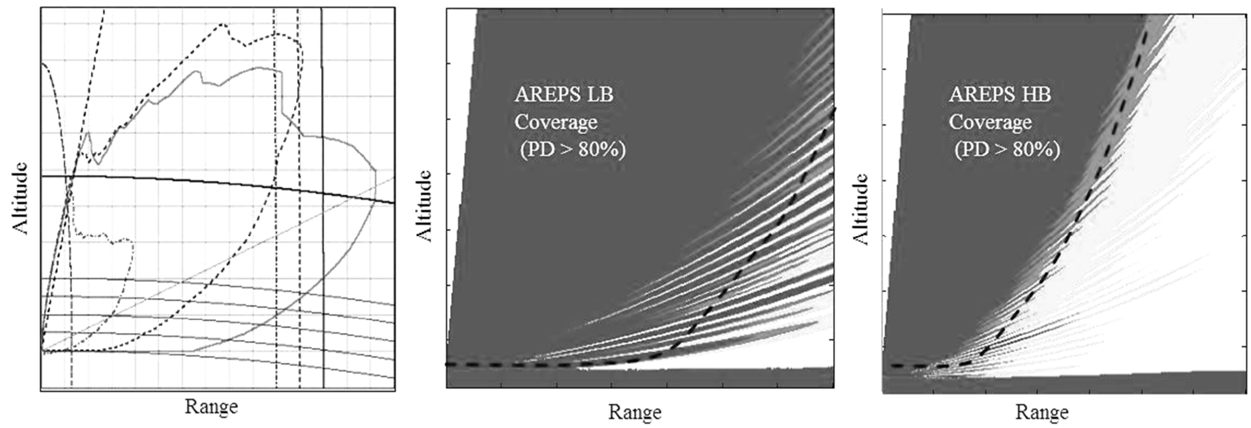

a) ASR-11 Vertical Coverage Diagram b) ASR-11 Low Beam Coverage (Model) c) ASR-11 High Beam Coverage (Model)

Figure 7: ASR-11 Model Verification to Vertical Coverage Diagram

In addition to collaborating on model development with Raytheon through our existing CRADA, we have been able to verify our modeling and simulation capability by comparing our modeling and simulation results to recently completed flight test scenarios (Drake, 2011). Results from Raytheon's CBP testing at Johnstown, PA indicate significant improvements in P_d from the baseline configuration (Drake, 2008). In addition, as part of our concept demonstrations for GBSAA, we have verified the modeling and simulation results for target detection and track initiation using instrumented flight scenarios near Edwards AFB during September 2011 and June 2012.

The intention of the field data collection was to compare radar surveillance data from a known instrumented target to the simulation results as an attempt to verify the accuracy of the modeling and simulation results. Additionally, we wanted to collect surveillance data to assess the radar performance of the ASR-11 in meeting GBSAA performance requirements. All of the flight scenarios were developed to probe the radar coverage and performance of the Edwards AFB ASR-11. These scenarios included approximately 80 hours of flight time in saw-tooth climb and descent switchback patterns with different orientations to the radar. Patterns in a North-South, East-West, and Northeast-Southwest orientation were conducted to adequately sample different target aspect angles relative to the fixed ASR-11 site. A sample of aircraft position data from a radar characterization pattern is provided in Figure 8.

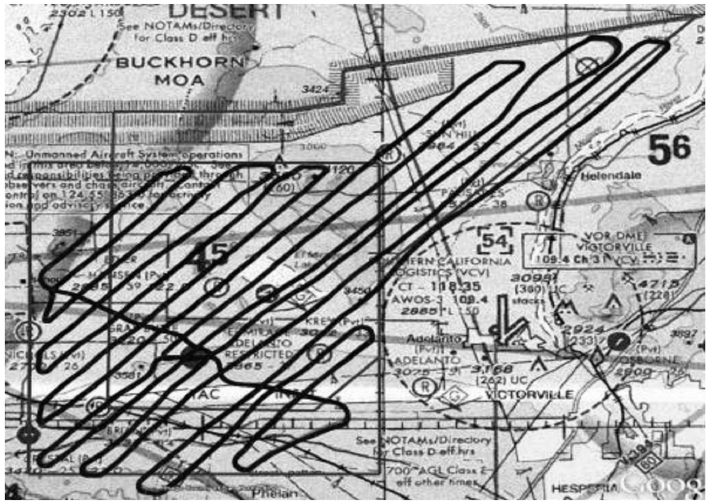

Figure 8: Northeast-Southwest Radar Characterization Pattern (target aircraft GPS data)

Data output from the modeling and simulation techniques discussed in this article includes a three-dimensional map of predicted probability of detections for the area surrounding Gray Butte Airfield near Edwards AFB CA. The detection probability results are specific to the Edwards ASR-11 radar characteristics (e.g. operating frequencies, tilt angle), the terrain profile of the area, the target radar cross section, and assumed standard day atmospheric conditions. The radar modeling technique produced probabilities of detection for points in space traversed by the target aircraft during the instrumented flight scenarios as well as distributions for track initiation time for the tracker settings used by the STARS LITE tracking system.

Since signal to noise ratio scales linearly with radar cross section, and the P_d versus SNR relationship is understood for the radar signal processing, the model output is in the form of P_d as a function of RCS and target location. Target location is an important factor, since the radar signal strength is subject to atmospheric conditions, range, propagation phenomenology, and terrain obscuration and scattering. The modeling and simulation results specific to the Edwards AFB ASR-11 were used to compare with the collected data from the flight scenarios.

The analysis of the collected aircraft truth data and radar data focused on the question of whether the model accurately predicted radar detection performance against a known target. The observed detection probability was determined by evaluating the number of reinforced (primary and secondary) radar returns compared with the number of secondary radar returns within the radar's line of sight and coverage area. Model detection probability is the aggregate of the simulation predicted detection probabilities at all points along the target aircraft trajectory that included a secondary radar return. The results for the different flight scenarios are depicted in Figure 9, with the dotted line denoting an exact match in aggregate detection probability. There is significant correlation between the model probabilities of detection and the observed reinforcement rates from the ASR-11 radar at Edwards AFB, with the highest deviation in detection probability being about three percentage points. Further investigation reveals that the missed detections were largely at locations in the periphery of the radar coverage, where the modeling and simulation analysis predicted low detection probabilities.

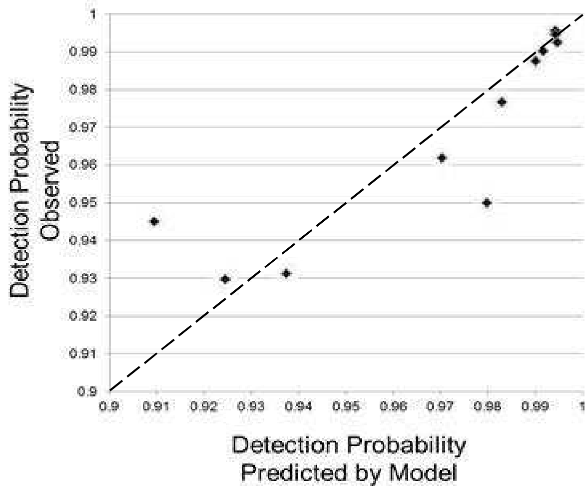

Figure 9: Observed versus Modeled Detection Probability for Gray Butte Scenarios

Currently, AREPS is limited in precisely modeling the user-specified antenna gain pattern by restricting the input to the same antenna pattern for receive and transmit. This limitation affects the accuracy of the ASR-11 model. However, adjustments to the model, coordinated with Navy SPAWAR and Raytheon, are believed to be a good approximation of the ASR-11 performance for the purposes of this study. Additionally, Navy SPAWAR is in the process of making enhancements to the surface clutter model, which may require modifications to the terrain classification and land cover algorithm approach provided in this article. We are coordinating with Navy SPAWAR on these changes.

B. Tracking System Modeling

Surveillance data from participating radar systems are correlated and fused in the tracking system. Target plots from different participating radars are correlated as a single plot if their reports are within the track correlation time constraint. That is, if multiple radar systems detect what the system determines to be the same target within a short period of time, the tracking system will correlate these target plots and fuse them as a single target plot. The objective of track initiation criteria is to establish a track on a series of successive positive target detections with a high confidence that the series of plots is representing a legitimate airborne target trajectory. Typically, successive target detections must meet an "*m* of *n* rule" for track initiation, where *m* is the number of positive hits, and *n* is the number of radar updates.

The objective of quickly initiating a track on a target is in direct competition with minimizing the false track rate. Appropriate track initiation parameter identification is important in maintaining a suitable balance between positive track initiation and the false track rate. The supplemental coverage from additional radar sources potentially reduces the time required for track initiation. Due to the asynchronous update rate experienced when surveillance data is fused from multiple radar systems, there will be times in which multiple radars detect a single target nearly simultaneously. These detections are correlated and counted as only one hit towards the *m* counter if the successive positive detections from the multiple radar systems occur within the same track correlation time constraint. Performing simulation trade studies on the tracking system logic and parameters can yield an optimized system for a given application.

C. Target Trajectory Generation

An air traffic characterization defines the performance characteristics of each of the intruding aircraft in the target generation model. During each simulation scenario, intruder flight performance is sampled from statistical distributions established from the airspace characterization. Using recorded radar data, we created statistical distributions of aircraft performance and operational behavior. We are particularly interested in modeling the behavior of non-cooperative aircraft as well as aircraft transmitting a VFR, non-discrete transponder beacon code (1200 code). Provided in Figure 10 a representative set of aircraft flight trajectories as well as aircraft velocity and climb rate distributions for non-cooperative and non-discrete (1200 code) aircraft.

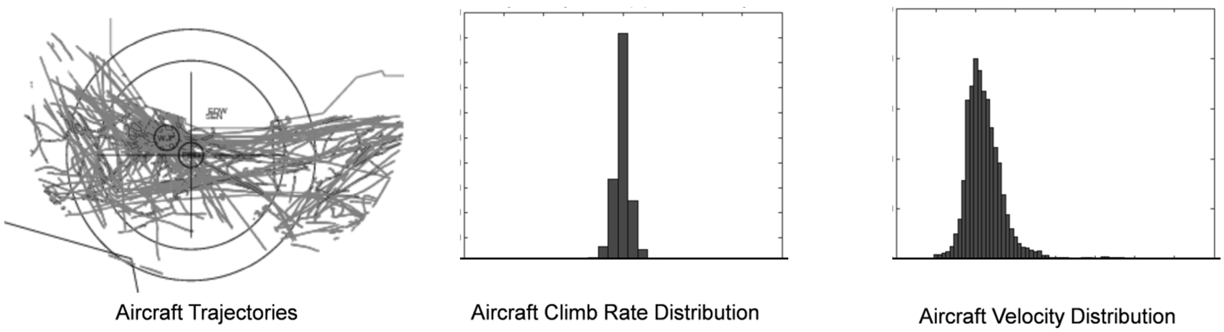

Figure 10: Non-cooperative and non-discrete (1200 code) aircraft trajectories and flight performance from airspace traffic characterization of Edwards AFB, March-May 2010

Intruder headings are randomly assigned and the altitude of the aircraft at the point of intrusion is defined as the bottom of the radar coverage beam at the location of intrusion. Since track initiation times are generally very short, we assume that there is no heading change, acceleration, or change in climb rate along the flight trajectory. The capability to model more dynamic intruder flight trajectories, which includes intruder acceleration / deceleration, turning, and changing climb rates, has been demonstrated but is not fully utilized.

D. Model Synthesis and Simulation

Detection time and track initiation time are difficult to evaluate analytically for scenarios when the radar P_d varies along the target trajectory and there are multiple radars covering the volume with different performance characteristics and asynchronous update rates. For a statistical distribution of target detection and track initiation times, simulating the performance and dynamics of the radar, tracker, and intruder aircraft is an attractive technical approach.

To evaluate target detection and track initiation times in an operational volume of interest, all target trajectories are generated such that they penetrate the radar coverage at the bottom of the beam. The elevation of the bottom of the radar beam is a function of the distance from the radar site due to the curvature of the earth and the local terrain due to line-of-sight obscuration, as well as the atmospheric conditions. Once the target penetrates the radar coverage, it will take some amount of time until the target is actually detected by a radar. This time is a function of the radar beam location at the time of intrusion, the radar update rate, and target P_d at the location of the intrusion and along the target trajectory (Brookner, 1998). The track initiation time is a function of the same factors as target detection but complicated by the issue of satisfying track initiation criteria (Brookner, 1998).

For each target intruder, the starting azimuth of each of the participating radar systems is randomly generated. At each time step in the simulation, the azimuth location of each of the radar beams and the location of the target intruder are updated. The simulation monitors the location of the intruder relative to the location of each of the radar sites, as well as the intruder latitude and longitude. When the radar beam is covering the intruder, the P_d at the specific azimuth, range, and altitude of the intruder is evaluated to establish a probabilistic radar detection hit or miss. The tracking model fuses the surveillance data from the different radar systems. Once track is initiated, in accordance with the defined track initiation logic and parameter settings, the simulation for the given intruder terminates and a new intruder scenario is generated. Results for each intruder scenario are recorded for post-processing analysis. To collect sufficient statistics to characterize system detection and tracking performance, simulation of ten million intruder scenarios are typically evaluated in a standard analysis.

IV. Results

The operational volume used for the GBSAA simulation scenario is a 4,000 nmi^2 area located in the vicinity of Edwards AFB, near Palmdale, California. Both an ASR-11 and a long range FPS-67B cover most of the operational volume. For the GBSAA case study, we simulated ten million pop-up aircraft intrusion scenarios uniformly distributed over the entire operational volume. We analyzed the spatially dependent simulation results to quantify system surveillance performance.

Three-dimensional radar coverage and detection performance, as a function of location relative to the radar site and target RCS, are determined from supplementary AREPS post-processing models that we have developed. In the case of multiple overlapping radar systems, the fused P_d for a given <latitude, longitude, altitude> can be estimated by appropriately combining each single radar P_d for that location. While this provides a reasonable estimate for overall surveillance coverage and performance, the radars are treated independently in all simulation studies.

Ten million pop-up intruders, modeled from statistical distributions of observed aircraft behavior in the area, were simulated in the Edwards operational volume to assess radar detection and tracking system performance. In areas close to the radar site where the SIR is high, and where the bottom of the coverage is provided by the ASR-11, the mean track initiation times are reasonably short. Within the ASR-11 coverage, mean track initiation times range from approximately 10 seconds in areas with very high P_d to 90 seconds in areas where P_d suffers due to various sources of signal degradation. For targets covered only by the FPS-67B, track initiation times suffer due to the long update rates of the long range radar. In regions where both the ASR-11 and FPS-67B are detecting the target intruder, track initiation times have the potential to be very low.

For the tracking system parameters used in the simulation, the theoretical minimum track initiation time is 4.8 seconds in areas where both an ASR-11 and FPS-67B are covering the airspace volume. From the simulation test case, the lowest observed track initiation time was 4.823 seconds. In this regard, simulation results match the expected outcome. In contrast, very high track initiation times can be expected in some extreme scenarios. For the purpose of identifying causes for high track initiation times, scenarios which resulted in unacceptably high track initiation times were flagged for closer inspection. High track initiation times can be explained by intruders that remain in a coverage void created by either terrain line-of-sight obscuration, multipath, or another source of interference. Also, some intruders penetrated the radar coverage but then exited the coverage, resulting in an inability for the system to initiate track. Target detection and track initiation time distributions vary widely across the operational volume due to variance in radar performance. Simulation results are consistent with the expected results.

After simulation results are fully collected, the performance of the radar and tracking system can be evaluated against the performance requirements needed by the architecture for safe UAS operations in the NAS. The results can be used to define safe UAS operating areas within an airspace volume of interest. The UAS must operate high enough above the bottom of the radar coverage to allow sufficient time for the radar and tracking system to detect and track non-cooperative intruders to avoid a collision hazard. A three-dimensional volume can be defined specifying areas within the operational volume which are not covered by a radar system, are within the buffer for track initiation, within the vertical separation requirements for the UAS, or adequate for GBSAA for UAS access to the NAS. Visualization through GoogleEarth and FalconView assist in the development of operational concepts and mission planning and execution, respectively.

V. Conclusions

Through this research effort, we have developed a high fidelity radar modeling and simulation capability to support analysis of a diverse set of ATM surveillance applications, including evaluating GBSAA for enabling UAS operations in the NAS. Our approach blends a series of supplementary models and simulation tools with AREPS. Radar performance information is integrated with a tracking system model and a target trajectory generator in a fast-time simulation architecture. The combined modeling and simulation approach enables radar detection, track initiation, and track maintenance simulations for evaluating system performance in detecting and tracking intruder aircraft.

We have enhanced the AREPS modeling capability through the development and integration of multiple supplementary modeling tools. Our front-end modeling enhancements include the development of a radar specification database, land type classification algorithm, and a land cover effects model. Land cover information is extracted from high-resolution satellite imagery, mapped to reflectivity coefficients, combined with terrain classification inference models, and imported into AREPS. The AREPS model uses radar platform specifications and calculates detection performance; taking into account atmospheric, environmental, terrain, and land cover effects. Radar platform specific models are used to generate radar operating curves, which reveal the platform specific trades between SIR, P_d, and P_{fa}. Radar performance information from AREPS for a given radar platform and site are coupled with the radar operating characteristics to evaluate the P_d as a function of location and target RCS. Radar coverage and detection performance can be visualized three-dimensionally and the data exported to support simulation studies.

Surveillance performance information from the radar modeling toolset integrates seamlessly into a simulation environment that combines radar performance with tracking algorithms and the generation of target trajectories from aircraft performance distributions. Target trajectories are generated and simulated throughout the operational volume. The tracking system fuses and correlates surveillance information of the simulated target intruders from all participating radar systems. These independent system models are simulated in fast time to evaluate target detection, track initiation, and track maintenance.

The modeling and simulation tool discussed in this paper has proven to be successful in providing an augmented understanding of the complex dynamics of the surveillance systems that perform the detection and tracking functions within the GBSAA architecture. Simulation experiments are used to evaluate system performance for planned UAS operating locations. The radar model provides three-dimensional radar coverage and P_d information throughout the operational volume, including spatially defined statistical distributions of track initiation times and altitudes for expected intruder aircraft. From these distributions, we can establish volumes of airspace in which the GBSAA architecture solution will provide adequate detection and tracking performance for UAS sense and avoid. Results enable concept of operation development, mission planning, and artifacts for supporting a UAS safety assessment.

Our current research has focused on using ground based radar systems to detect and track non-cooperative aircraft for UAS Sense and Avoid. Each of the targets have a flight trajectory generated by sampling representative distributions of GA aircraft performance in the airspace of interest. However, one underlying assumption is that all targets, regardless of size or type, have an RCS of $1m^2$. While an RCS of $1m^2$ has historically been accepted as adequate for civilian aircraft with a single human occupant, it is advantageous to evaluate the track initiation times for other targets. Thus, a more comprehensive model that will have representative joint distributions for target RCS and vehicle performance is currently under development. The limiting factor behind the development of this enhanced model is not the radar performance modeling, but the development of an intruder database with accurate aspect dependent RCS distributions. This will be an important step in supporting a safety case for UAS operations in the NAS as well as other applications.

Our plans for future modeling and simulation applications include evaluating alternative sense and avoid architecture solutions with different radar surveillance systems and tracking system logic. In addition, we have recently become interested in quantitatively assessing the impact that wind farms, large solar arrays, and other disruptive structures have on the performance of primary radar systems. Due to their very nature, these impacts are highly site specific. We believe that we can leverage our modeling and simulation capability, with its ability to take into account terrain and land cover effects, to evaluate these impacts. We have completed preliminary modeling and simulation studies to evaluate the performance benefits of concurrent beam processing in the ASR-11. This radar signal-processing enhancement shows promise in improving P_d and enabling altitude estimation for primary targets. Additional modeling and simulation trade studies are required to evaluate these alternative considerations comprehensively.

Acknowledgments

The authors would like to gratefully acknowledge MITRE colleagues Dr. Ken Hsu, and Dr. Bette Winer for their expertise in radar and tracking system modeling, Dr. Steve Bowling for his probability of detection insights and suggestions, and Shawn Hanegan for summarizing the flight validation results. We would like to acknowledge the sponsoring organization, The United States Air Force (AFLCMC/HBAI) and the valuable operational insights from Captain Robert Walker (USAF). Members from our MITRE UAS integration team including Roger Francis, Bill Hershey, Chris Jella, and Marie Miller motivated this research. We would also like to acknowledge Peter Drake, Dr. Francis Lok, and Robert Stamm from the Raytheon Corporation for their technical assistance in modeling the ASR-11 radar system. Without their knowledge, technical contributions, and guidance, this research would not have been possible.

References

1. Austin, R. (2010), *Unmanned Aircraft Systems,* American Institute of Aeronautics and Astronautics, John Wiley & Sons, Blacksburg, VA .

2. Barton, D.K, (1988), *Modern Radar System Analysis,* Artech House, Boston, MA.

3. Brookner, E. (1998), *Tracking and Kalman Filtering Made Easy,* John Wiley & Sons Inc., New York, NY .

4. Drake, P. (2011), *Overview of Raytheon Wind Farm Mitigation Techniques and Test Results,* CNS/ATM Conference, Orlando, FL.

5. Drake, P. and Lok, F. Y. (2009) *Raytheon Windfarm Mitigation*, Raytheon Corporation, Marlborough, MA.

6. Federal Aviation Administration (2010), *Federal Aviation Regulations (FAR/AIM)*, Department of Transportation.

7. Federal Aviation Administration (2009), *Sense and Avoid (SAA) for Unmanned Aircraft Systems (UAS)*, Department of Transportation.

8. Homer, C. H., Fry, J. A., Barnes, C. A. (2012), *The National Land Cover Database, US Geological Survey Fact Sheet 2012-3200.*

9. Long, M. W. (2001), *Radar Reflectivity of Land and Sea,* Artech House, 3rd Ed., Boston, MA.

10. Mahafza, B. R. and Elsherbeni, A. Z. (2004), MATLAB *Simulations for Radar System Design*, Chapman & Hall/CRC, Boca Raton, FL.

11. Nolan, M. S. (2011), *Fundamentals of Air Traffic Control*, Delmar Cenage Learning, Clifton Park, NY .

12. O'Donnell, R. M. (2010), Radar Systems Engineering: Detection of Signals in Noise, IEEE.

13. Patterson, W. L. (2007), *EM Propagation Modeling and System Performance Assessment by SPAWARSYSCEN San Diego* , 9th International Symposium on Advanced Radio Technologies, Boulder, CO.

14. Raytheon Corporation (2011), ASR-11/AN/GPN-30 Digital Airport Surveillance Radar (DASR), [Online] .

15. Richards, M. A., Scheer, J. A. and Holm, W. A. (2010), *Principles of Modern Radar*, Scitech Publishing Inc., Raleigh, NC .

16. Skolnik, M. (1990), *Radar Handbook, 2nd Ed.*, McGraw-Hill, Inc, New York, NY.

17. Skolnik, M. (2008), *Radar Handbook, 3rd Ed.*, McGraw-Hill Inc, New York, NY.

18. Space and Naval Warfare Systems Center (SPAWAR) (2010), *Advanced Refractive Effects Prediction System*, [Online], https://nmso.navy.mil/view_detail.cfm?RID=DTS_N_1000714..

19. Space and Naval Warfare Systems Center, Pacific Atmospheric Propagation Branch (5548) (2009), *User's Manual (UM) for Advanced Refractive Effects Prediction System, umAREPS-37,* San Diego, CA.

20. Weibel, R., et al. (2011), *Establishing a Risk-Based Separation Standard for Unmanned Aircraft Self Separation,* MIT Lincoln Laboratory, Lexington, MA.

21. Wood, J. (1996), *The Geomorphological Characterization of Digital Elevation Models,*PhD Thesis, University of Leicester, UK,.